International Journal of
Mathematical Modelling & Computations
Vol. 10, No. 03, Summer 2020, 161- 177

A Model of Coronavirus Pandemic Spread with Lockdown and Quarantine

D. K. Mamo*
Department of Mathematics, College of Natural and Computational Sciences, Debre Berhan University, P.O.Box 445, Debre Berhan, Ethiopia.

Abstract. Globally emerged Corona Virus Disease (COVID-19), has generated multiple damages in the worldwide community and caused enormous mortality. In this paper, a researcher develops *SLEAIQRD* (Susceptible-Lockdown-Exposed-Asymptomatic-Symptomatic-Quarantine-Recovery-Death) COVID-19 spread model. The disease-free equilibrium globally asymptotically stable when $R_0 \leqslant 1$. And also endemic equilibrium stable whenever $R_0 > 1$. COVID-19 spread dies out when $R_0 \leqslant 1$, while the spread continue in the community when $R_0 > 1$. For the lockdown intervention measure, at least 30% of coverage and competence needed to mitigate and control COVID-19 spread. Early identification, quarantine suspected peoples, quickly laboratory tests, and isolation of contagious individuals are inherent for COVID-19 containment. The researcher's conclusion suggests that high coverage of the contact tracing process is vital to stop the pandemic outbreak. Further curiously, beyond 60% exposed quarantine and a minimum of 50% isolation of infectious individuals overcome the burden and begin to control the COVID-19 outbreak. Numerical solutions strengthen the theoretical analysis.

Received: 10 March 2020, Revised: 19 April 2020, Accepted: 30 April 2020.

Keywords: COVID-19; Lockdown; Quarantine; Stability analysis; Numerical result.

AMS Subject Classification: 34D20, 34D23, 65L12, 92D30.

Index to information contained in this paper

1. Introduction

Globally emerged Corona Virus Disease(COVID-19) caused by severe acute respiratory syndrome coronavirus 2 (SARS-CoV-2) originated from a wet market in

*Corresponding author. Email: ketemadejen@gmail.com

http://ijm2c.iauctb.ac.ir

Wuhan, China, is now widespread in the world and has severely affected many counties. [17] [18]. It has generate multiple damages in worldwide community and caused enormous mortality. The most common symptoms of COVID-19 are fever, tiredness, and dry cough. Some patients may have aches and pains, nasal congestion, runny nose, sore throat or diarrhea. These symptoms may appear 2-14 days after exposure, most commonly around five days [16, 19].

People infected by those initial cases spread the disease to other drastically due to human to human transmission [15]. Although Corona represents a major public health issue in world, as of March 11, 2020, over 118,000 infections spanning 113 countries have been confirmed by the World Health Organization (WHO). The WHO declared this public health emergency as a pandemic [9]. As of 14 April 2020, WHO reported $1,844,863$ confirmed case and $117,021$ deaths have been recorded globally [5].

Mathematical modeling based on system of differential equations may provide a comprehensive mechanism for the dynamics of a disease transmission. The study about the spread and control of COVID-19 is essential at this time. Different scholars are study about infectious disease spread control by using modeling approach [1–3, 7, 8, 10]. Recently, researcher study a bout COVID-19 [4, 11, 13, 20]. The present work is $SEIR$ form [12], which incorporates the recommended public health interventions in the current pandemic. The recommended mitigation strategies of the pandemic are lockdown, quarantine, and isolation of infected individuals by efficient identification process. A researcher focus on the impact of intervention measures by varying the parameter values. The model result indicates that the containment of the pandemic requires high level of both identification and separation of infected individuals from the susceptible population.

2. Model formulation

In this model, consider $N(t)$ be the total population at any time t, and divided into eight sub-populations.

- $S(t)$- susceptible population, which denotes individuals who are susceptible to get the virus and so might become infectious when exposed at a time t.
- $L(t)$- lockdown population, which represents some portion of the susceptible population those are ordered at-home quarantined.
- $E(t)$- exposed population, which denotes the individuals who are COVID-19 infected, yet not contagious at a time t.
- $A(t)$- asymptomatic infected population, which represents contagious individuals, who don't exhibit COVID-19 related symptoms at a time t
- $Q(t)$- quarantine population, which denotes individuals who are suspected by COVID-19 becomes under quarantine at a time t.
- $I(t)$- symptomatic infected population, which denotes contagious individuals those were manifested COVID-19 related symptoms at a time t.
- $R(t)$- recovered population, which represents the number of COVID-19 discharged individuals at a time t.
- $D(t)$- deceased population, which represents the number of COVID-19 induced death.

The model schematic diagram describes in Figure 1.

In the process of COVID-19 spreading, the spreading among these eight states is governed by the following assumptions. It is assumed that β is the contact rate of susceptible individuals with spreaders and the disease transmission follows the mass action principle. The transmission contribution of asymptomatic infected is

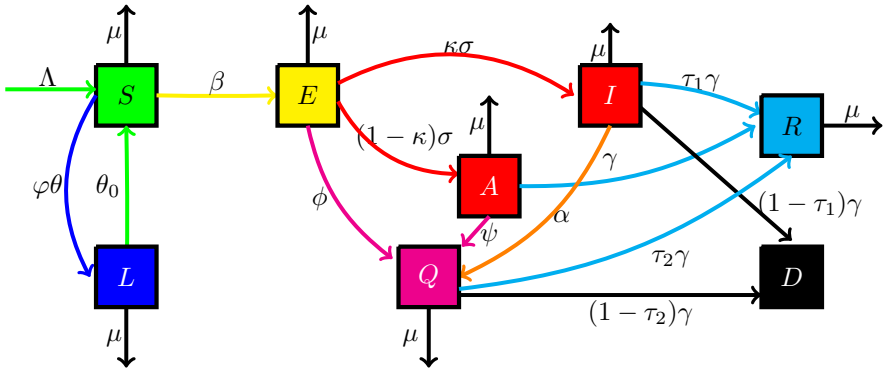

Figure 1. Schematic diagram of the model.

adjusted by the parameter η.

It is assumed that some portion of susceptible can be at-home quarantine order by the rate of θ, those are avoiding contact with the infected individual to protect themselves. The parameter φ is a measure of the accuracy of stay-at-home order. Considering lockdown lifting rate is θ_0 (so $1/\theta_0$ is lockdown period). The one who completed incubation period becomes to infected at a rate of σ, that means $\frac{1}{\sigma}$ is the average duration of incubation. Moreover, the exposed population changed to symptomatic by the probability of κ. By early identification and symptom manifestation exposed, symptomatic and asymptomatic individuals becomes to quarantine at a rate of ϕ, α, and ψ respectively. It is assumed that the infectious infected individuals, leading to disease prevalence. The average duration of infectiousness is $\frac{1}{\gamma}$, when γ is the transmission rate from infected to recovery or death.In my assumption recovery from quarantined is better than and symptomatic class due to clinical treatment. Symptomatic infected and quarantine are recover with a probability of τ_1 and τ_2, and also they will becomes to death with a probability of $(1-\tau_1)$ and $(1-\tau_2)$ respectively. The parameter Λ is the recruitment, while μ natural birth and death rate of each state individuals. The parameters are all non-negative.

Based on the above considerations, the pandemic spreading leads to dynamic transitions among these states, shown in Figure 1. Taking into account the above circumstances, the dynamics of COVID-19 outbreak is governed by the following system of nonlinear ordinary differential equations:

$$\begin{aligned}
\frac{dS}{dt} &= \Lambda - \beta S(t)\left(I(t) + \eta A(t)\right) - (\mu + \varphi\theta)S(t) + \theta_0 L(t),\\
\frac{dL}{dt} &= \varphi\theta S(t) - (\theta_0 + \mu)L(t),\\
\frac{dE}{dt} &= \beta S(t)\left(I(t) + \eta A(t)\right) - (\phi + \sigma + \mu)E(t),\\
\frac{dA}{dt} &= (1-\kappa)\sigma E(t) - (\psi + \gamma + \mu)A(t),\\
\frac{dI}{dt} &= \kappa\sigma E(t) - (\alpha + \gamma + \mu)I(t),\\
\frac{dQ}{dt} &= \phi E(t) + \psi A(t) + \alpha I(t) - (\gamma + \mu)Q(t),\\
\frac{dR}{dt} &= \gamma A(t) + \tau_1\gamma I(t) + \tau_2\gamma Q(t) - \mu R(t),\\
\frac{dD}{dt} &= (1-\tau_1)\gamma I(t) + (1-\tau_2)\gamma Q(t) - \mu D(t)
\end{aligned} \tag{1}$$

The total population $N(t)$ would be a constant all the time in this model i.e.,

$$N(t) = S(t) + L(t) + E(t) + I(t) + A(t) + Q(t) + R(t).$$

Assumed the total population is normalized and it's equals to one. We have the non-negative initial conditions

$$(S(0), L(0), E(0), I(0), Q(0), A(0), R(0), D(0)) \in \mathbb{R}^8_+. \tag{2}$$

3. Mathematical analysis of the model

Proposition 3.1 The biologically feasible region

$$\Omega = \{(S, L, E, A, Q, I, R) \in \mathbb{R}^8_+ : 0 < S + L + E + I + A + Q + R \leqslant \frac{\Lambda}{\mu}\}$$

is a positively invariant and attracting region for the disease transmission model given by system (1) with initial conditions equation (2).

Proof Summing up the eight equations in system (1) and denoting

$$N(t) = S(t) + L(t) + E(t) + I(t) + A(t) + Q(t) + R(t)$$

we get

$$\frac{dN(t)}{dt} \leqslant \Lambda - \mu N(t) - \mu D(t).$$

This implies that

$$\frac{dN(t)}{dt} + \mu N(t) \leqslant \Lambda.$$

Now, integrating both sides of the above inequality, we obtain

$$0 < N(t) \leqslant \left(N(0)e^{-\mu t} + \frac{\Lambda}{\mu}(1 - e^{-\mu t}) \right).$$

$N(t)$ approaches to $\frac{\Lambda}{\mu}$, whenever $t \to \infty$, this implies that $N(t) \leqslant \frac{\Lambda}{\mu}$. Thus, the set Ω is positive invariant, that is, all initial solutions belong to Ω remain in Ω, $\forall t > 0$. ■

Hence, system (1) is considered mathematically and biologically well posed in Γ[21].

3.1 *Equilibrium analysis*

In this subsection, we show the feasibility of all equilibria by setting the rate of change with respect to time t of all dynamical variables to zero. The model (1) has two feasible equilibria, which are listed as follows:

(i) Disease-free equilibrium (DFE) $E_0 \left(\frac{\Lambda(\theta_0+\mu)}{\mu(\varphi\theta+\theta_0+\mu)}, \frac{\Lambda\varphi\theta}{\mu(\varphi\theta+\theta_0+\mu)}, 0, 0, 0, 0, 0, 0 \right)$.

(ii) Endemic equilibrium (EE) E^* (S^*, L^*, E^*, A^*, I^*, Q^*, R^*, D^*).

The existence of endemic equilibrium is computed after we have the basic reproductive number $\mathcal{R}_0$.

3.1.1 Basic reproduction number

Here, we will find the basic reproduction number ($\mathcal{R}_0$) of the model (1) using next generation matrix approach [14]. We have the matrix of new infection $\mathcal{F}(X)$ and the matrix of transfer $\mathcal{V}(X)$. Let $X = (E,\, A,\, I,\, Q,\, L,\, S,\, R,\, D)^T$, the model (1) can be rewritten as:

$$\frac{dX}{dt} = \mathcal{F}(X) - \mathcal{V}(X),$$

where

$$\mathcal{F}(X) = \begin{pmatrix} \beta S(t)\left(I(t) + \eta A(t)\right) \\ 0 \\ 0 \\ 0 \\ 0 \\ 0 \\ 0 \\ 0 \end{pmatrix},$$

$$\mathcal{V}(X) = \begin{pmatrix} B_3 E(t) \\ B_4 A(t) - (1-\kappa)\sigma E(t) \\ B_5 I(t) - \kappa\sigma E(t) \\ B_6 Q(t) - \phi E(t) - \psi A(t) - \alpha I(t) \\ B_2 L(t) - \varphi\theta S(t) \\ \beta S(t)\left(I(t) + \eta A(t)\right)) + B_1 S(t) - \Lambda - \theta_0 L(t) \\ \mu R(t) - \gamma A(t) - \tau_1\gamma I(t) - \tau_2\gamma Q(t) \\ \mu D(t) - (1-\tau_1)\gamma I(t) - (1-\tau_2)\gamma Q(t) \end{pmatrix},$$

where, $B_1 = (\mu + \varphi\theta)$, $B_2 = (\theta_0 + \mu)$, $B_3 = (\phi + \sigma + \mu)$, $B_4 = (\psi + \omega + \gamma + \mu)$, $B_5 = (\alpha + \gamma + \mu)$, $B_6 = (\gamma + \mu)$.

The Jacobian matrices of $\mathcal{F}(X)$ and $\mathcal{V}(X)$ at the disease free equilibrium $E_0\left(\frac{\Lambda(\theta_0+\mu)}{\mu(\varphi\theta+\theta_0+\mu)}, \frac{\Lambda\varphi\theta}{\mu(\varphi\theta+\theta_0+\mu)}, 0, 0, 0, 0, 0, 0\right)$ are, respectively,

$$J\mathcal{F}(E_0) = \begin{pmatrix} F & 0 \\ 0 & 0 \end{pmatrix}, \text{ and } J\mathcal{V}(E_0) = \begin{pmatrix} V & 0 \\ J_1 & J_2 \end{pmatrix}.$$

$$F = \begin{pmatrix} 0 & \eta A_1 & A_1 & 0 \\ 0 & 0 & 0 & 0 \\ 0 & 0 & 0 & 0 \\ 0 & 0 & 0 & 0 \end{pmatrix} \text{ and } V = \begin{pmatrix} B_3 & 0 & 0 & 0 \\ (\kappa-1)\sigma & B_4 & 0 & 0 \\ -\kappa\sigma & 0 & B_5 & 0 \\ -\phi & -\psi & -\alpha & B_6 \end{pmatrix},$$

where, $A_1 = \beta\Lambda\frac{\mu+\theta_0}{\mu(\mu+\varphi\theta+\theta_0)}$.

The inverse of V is computed as

$$V^{-1} = \begin{pmatrix} \frac{1}{B_3} & 0 & 0 & 0 \\ \frac{\sigma B_5 B_6 - \kappa\sigma B_5 B_6}{B_3 B_4 B_5 B_6} & \frac{1}{B_4} & 0 & 0 \\ \frac{\kappa\sigma}{B_3 B_5} & 0 & \frac{1}{B_5} & 0 \\ \frac{\alpha\kappa\sigma B_4 + \phi B_5 B_4 - \kappa\sigma\psi B_5 + \sigma\psi B_5}{B_3 B_4 B_5 B_6} & \frac{\psi}{B_4 B_6} & \frac{\alpha}{B_5 B_6} & \frac{1}{B_6} \end{pmatrix}.$$

The next generation matrix is computed as

$$F \times V^{-1} = \begin{pmatrix} \frac{\eta(\sigma B_5 B_6 - \kappa\sigma B_5 B_6)A_1}{B_3 B_4 B_5 B_6} + \frac{\kappa\sigma A_1}{B_3 B_5} & \frac{\eta A_1}{B_4} & \frac{A_1}{B_5} & 0 \\ 0 & 0 & 0 & 0 \\ 0 & 0 & 0 & 0 \\ 0 & 0 & 0 & 0 \end{pmatrix}.$$

The spectra radius of next generation matrix is

$$\rho(FV^{-1}) = \frac{\sigma A_1 \left((1-\kappa)B_5\eta + B_4\kappa + (1-\kappa)\omega\right)}{B_3 B_4 B_5}.$$

Hence, the basic reproduction number is

$$\mathcal{R}_0 = \frac{\sigma A_1 \left((1-\kappa)(B_5\eta + \omega) + B_4\kappa\right)}{B_3 B_4 B_5}.$$

3.1.2 Stability of the disease free equilibrium

In this subsection, a researcher shows linear stability of E_0 by finding the sign of eigenvalues of the Jacobian matrix of the model (1).

Theorem 3.1 If $\mathcal{R}_0 < 1$, the disease-free equilibrium E_0 of system (1) is locally asymptotically stable, and it is unstable if $\mathcal{R}_0 > 1$.

Proof In the absence of the disease, the model has a unique disease free equilibrium E_0. Now the Jacobian matrix at equilibrium E_0 is given by:

$$\begin{pmatrix} -B_1 & \theta_0 & 0 & -\eta A_1 & -A_1 & 0 & 0 & 0 \\ \varphi\theta & -B_2 & 0 & 0 & 0 & 0 & 0 & 0 \\ 0 & 0 & -B_3 & \eta A_1 & A_1 & 0 & 0 & 0 \\ 0 & 0 & (1-\kappa)\sigma & -B_4 & 0 & 0 & 0 & 0 \\ 0 & 0 & \kappa\sigma & \omega & -B_5 & 0 & 0 & 0 \\ 0 & 0 & \phi & \psi & \alpha & -B_6 & 0 & 0 \\ 0 & 0 & 0 & \gamma & \gamma\tau_1 & \gamma\tau_2 & -\mu & 0 \\ 0 & 0 & 0 & 0 & \gamma(1-\tau_1) & \gamma(1-\tau_2) & 0 & -\mu \end{pmatrix}. \tag{3}$$

Here, we need find the eigenvalue of the system from the Jacobian matrix (3). We obtain the characteristic polynomial

$$P(\lambda) = (-B_6 - \lambda)(-\lambda - \mu)^2 \left(\lambda^2 + (B_1 + B_2)\lambda + B_1 B_2 - \varphi\theta\theta_0\right)\left(\lambda^3 + c_1\lambda^2 + c_2\lambda + c_3\right). \tag{4}$$

where, $c_1 = (B_3 + B_4 + B_5)$, $c_2 = (B_3 B_4(1 - \mathcal{R}_a) + B_3 B_5 + B_4 B_5)$, and $c_3 = B_3 B_4 B_5(1 - \mathcal{R}_0)$.

From the characteristic polynomial in equation (4), it is easy to get three real negative eigenvalues of $J(E_0)$, which are $\lambda_{1,2} = -\mu$, and $\lambda_3 = -B_6$. We get the other real negative eigenvalues from the expression

$$\lambda^2 + (B_1 + B_2)\,\lambda + B_1B_2 - \varphi\theta\theta_0 \tag{5}$$

and

$$\lambda^3 + c_1\lambda^2 + c_2\lambda + c_3. \tag{6}$$

From the quadratics equation (5), $(B_1 + B_2) > 0$ and also $B_1B_2 - \varphi\theta\theta_0 > 0$. This implies that the eigenvalues $\lambda_{4,5}$ are negative. Again from the polynomial (6), we have negative real root $\lambda_{6,7,8}$, whenever $\mathcal{R}_0 < 1$. Thus, the equilibrium E_0 is locally asymptotically stable if $\mathcal{R}_0 < 1$. E_0 becomes unstable whenever E^* is feasible (i.e., $\mathcal{R}_0 > 1$). The proof is complete. ■

Physically speaking, Theorem 3.1 implies that disease can be eliminated if the initial sizes are in the basin of attraction of the DFE E_0. Thus the infected population can be effectively controlled if $\mathcal{R}_0 < 1$. To ensure that the effective control of the infected population is independent of the initial size of the human population, a global asymptotic stability result must be established for the DFE.

Theorem 3.2 If $\mathcal{R}_0 \leqslant 1$, then the disease-free equilibrium, E_0, of system (1) is globally asymptotically stable in Ω.

Proof To show the global stability of the disease-free equilibrium E_0, we construct the following Lyapunov function Let $Z = (S, L, E, A, I, Q, R, D)^T$ and consider a Lyapunov function,

$$\mathcal{J}(Z) = a_1E + a_2A + a_3I$$

in which we only considered the variables representing the infected components of the model, where, $a_1 = \sigma(\kappa B_4 + \eta(1-\kappa)B_5)/B_3B_4$, $a_2 = \eta B_5/B_4$ and $a_3 = 1$.

Differentiating $\mathcal{J}$ in the solutions of system (1) we get

$$\begin{aligned}
\dot{\mathcal{J}} &= a_1\dot{E} + a_2\dot{A} + a_3\dot{I},\\
&= \frac{\sigma(\kappa B_4 + \eta(1-\kappa)B_5)}{B_3B_4}\left(\beta S(t)\left(I(t) + \eta A(t)\right) - B_3E(t)\right)\\
&\quad + \frac{\eta B_5}{B_4}\left((1-\kappa)\sigma E(t) - B_4A(t)\right) + \kappa\sigma E(t) + -B_5I(t)\\
&= B_5\frac{\sigma(\kappa B_4 + \eta(1-\kappa)B_5)}{B_3B_4B_5}\beta S(t)\left(I(t) + \eta A(t)\right) - B_5(I(t) + \eta A(t))\\
&= \left(\frac{\sigma(\kappa B_4 + \eta(1-\kappa)B_5)}{B_3B_4B_5}\beta S(t) - 1\right)B_5(I(t) + \eta A(t)).
\end{aligned}$$

Therefore,

$$\begin{aligned}
\dot{\mathcal{J}} &\leqslant \left(\frac{\sigma(\kappa B_4 + \eta(1-\kappa)B_5)}{B_3B_4B_5}\beta S(0) - 1\right)B_5(I(t) + \eta A(t))\\
&= (\mathcal{R}_0 - 1)B_5(I(t) + \eta A(t)),
\end{aligned}$$

since $S(t) \leqslant S(0)$ and $S(t) \in \Omega$.
$\dot{\mathcal{J}} < 0$ whenever $\mathcal{R}_0 < 1$. Furthermore, $\dot{\mathcal{J}} = 0$ if and only if $\mathcal{R}_0 = 1$. Thus the largest invariant set in $\left\{ Z \in \Omega | \dot{\mathcal{J}}(E, A, I) = 0 \right\}$ is the singleton of E_0. By LaSalle's Invariance Principle the disease-free equilibrium is globally asymptotically stable in Ω, completing the proof. ■

Theorem 3.2 completely determines the global dynamics of model (1) in when $\mathcal{R}_0 \leqslant 1$. It establishes the basic reproduction number $\mathcal{R}_0$ as a sharp threshold parameter. Namely, if $\mathcal{R}_0 < 1$, all solutions in the feasible region converge to the DFE E_0, and the disease will die out from the community irrespective of the initial conditions. If $\mathcal{R}_0 > 1$, E_0 is unstable and the system is uniformly persistent, and a disease spread will always exist.

3.1.3 Endemic equilibrium and its stability

Here, we show the existence and uniqueness of endemic equilibrium E^*. The values of $S^*, L^*, E^*, A^*, I^*, Q^*, R^*$ and D^* are obtained from the system (1), we get

$$S^* = \frac{\Lambda(\mu+\theta_0)}{\mathcal{R}_0\mu(\mu+\theta_0+\varphi\theta)},\ L^* = \frac{\Lambda\varphi\theta}{\mathcal{R}_0},\ E^* = \frac{\Lambda(\mathcal{R}_0-1)}{B_3\mathcal{R}_0},\ A^* = \frac{\Lambda\sigma(1-\kappa)(\mathcal{R}_0-1)}{B_3B_4\mathcal{R}_0},$$
$$I^* = \frac{\kappa\Lambda\sigma(\mathcal{R}_0-1)}{B_3B_5\mathcal{R}_0},\ Q^* = \frac{\phi E^* + \psi A^* + \alpha I^*}{B_6},\ R^* = \frac{\gamma A^* + \tau_1\gamma I^* + \tau_2\gamma I^*}{\mu},$$
$$D^* = \frac{(1-\tau_1)\gamma I^* + (1-\tau_2)\gamma I^*}{\mu}.$$

We obtain a unique positive endemic equilibrium E^*, when $\mathcal{R}_0 > 1$.

Theorem 3.3 If $\mathcal{R}_0 > 1$, then the endemic equilibrium point E^* of system (1) is locally asymptotically stable.

Proof The Jacobian matrix of the model at E^* is

$$\begin{pmatrix} -B_1-H_1 & \theta_0 & 0 & -\eta D_1 & -D_1 & 0 & 0 & 0 \\ \theta & -B_2 & 0 & 0 & 0 & 0 & 0 & 0 \\ H_1 & 0 & -B_3 & \eta D_1 & D_1 & 0 & 0 & 0 \\ 0 & 0 & (1-\kappa)\sigma & -B_4 & 0 & 0 & 0 & 0 \\ 0 & 0 & \kappa\sigma & \omega & -B_5 & 0 & 0 & 0 \\ 0 & 0 & \phi & \psi & \alpha & -B_6 & 0 & 0 \\ 0 & 0 & 0 & \gamma & \gamma\tau_1 & \gamma\tau_2 & -\mu & 0 \\ 0 & 0 & 0 & 0 & \gamma(1-\tau_1) & \gamma(1-\tau_2) & 0 & -\mu \end{pmatrix} \tag{7}$$

where $H_1 = (I^* + \eta A^*)$, and $D_1 = \beta S^*$.

From the Jacobian matrix (7) easily to get $\lambda_{1,2} = -\mu, \lambda_3 = -B_6$ and the other eigenvalues of the system needs further finding. The characteristic polynomial of (7) is

$$P(\lambda) = \lambda^5 + a_1\lambda^4 + a_2\lambda^3 + a_3\lambda^2 + a_4\lambda + a_5 = 0. \tag{8}$$

Where

$$
\begin{aligned}
a_1 &= B_1 + B_2 + B_3 + B_4 + B_5 + H_1 \\
a_2 &= (B_1 + B_2 + H_1)(B_3 + B_4 + B_5) \\
a_3 &= (B_1 + B_2)(B_3B_4 + B_3B_5 + B_4B_5) + B_2H_1(B_3 + B_4 + B_5) + B_4B_5H_1 \\
a_4 &= B_2H_1(B_3B_4 + B_3B_5 + B_4B_5) + A_1\sigma((1-\kappa)\eta + \kappa)\theta\varphi\theta_0 \\
a_5 &= B_3B_4B_5\varphi\theta\theta_0(\mathcal{R}_0 - 1).
\end{aligned} \tag{9}
$$

The polynomial (8) has negative roots (eigenvalues) if all its coefficients terms are positive, or it satisfies Routh-Hurwitz criteria of stability [6]. From (9) we can verify that $\forall a_i > 0$, $i = 1, 2, 2, 3, 4, 5$ when $\mathcal{R}_0 > 1$. And also, $a_1a_2a_3 > a_3^2 + a_1^2a_4$, $(a_1a_4 - a_5)\left(a_1a_2a_3 - a_3^2 - a_1^2a_4\right) > a_5\left(a_1a_2 - a_3\right)^2 + a_1a_5^2$. Therefore, according to the Routh-Hurwitz criterion, we can get that all the roots of the above characteristic equation have negative real parts. Thus, the endemic equilibrium asymptotically stable. The proof is complete. ■

The local stability analysis of the endemic equilibrium tells that if the initial values of any trajectory are near the equilibrium E^*, the solution trajectories approach to the equilibrium E^* under the condition $\mathcal{R}_0 > 1$. Thus, the initial values of the state variables S, L, E, A, I, Q, R and D are near to the corresponding equilibrium levels, the equilibrium number of infected individuals get stabilized if $\mathcal{R}_0 > 1$.

3.2 *Sensitivity analysis*

Sensitivity analysis is used to identify parameters that have a tremendous impact on $\mathcal{R}_0$ and should be targeted by intervention strategies. More precisely, graphical displays allow measuring the relative change in a $\mathcal{R}_0$ when a parameter changes. Epidemiological characteristics of COVID-19 quantify by some parameters, which are averagely fixed. The remaining parameters are varying, which used to determines the status of the pandemic outbreak. The normalized sensitivity index Υ_λ is given by

$$
\Upsilon_\lambda^{\mathcal{R}_0} = \frac{\partial \mathcal{R}_0}{\partial \lambda} \times \frac{\lambda}{\mathcal{R}_0}.
$$

The researcher focuses on varying parameter values, which involve $\mathcal{R}_0$ expression, and their sensitivity will be described below.

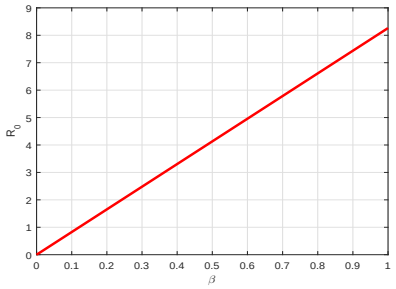

Figure 2. $\mathcal{R}_0$ vs the parameter β.

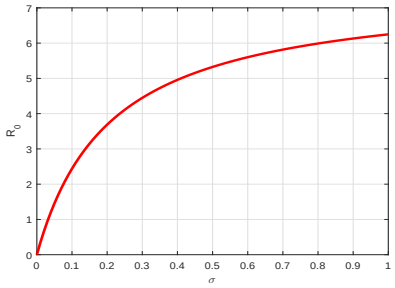

Figure 3. $\mathcal{R}_0$ vs the parameter σ.

A researcher can find some interesting results, which have been showed in Figures 2 and 3, it can be seen that big β or σ can lead to large $\mathcal{R}_0$. That is to say, the larger contact or short incubation period can increase the opportunity of disease

spreading. If we reduce the transmission rate by quarantine or any appropriate control measure, then the disease outbreak will end.

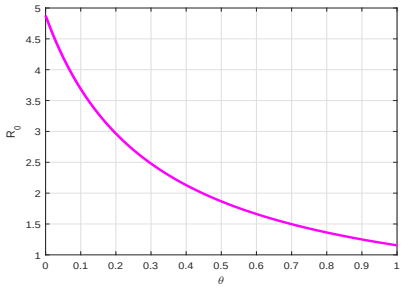

Figure 4. $\mathcal{R}_0$ vs the parameter θ.

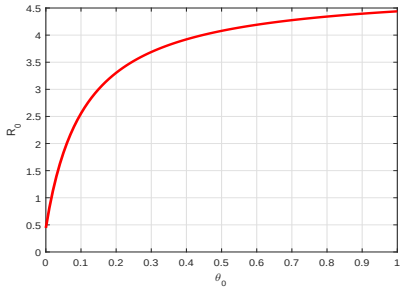

Figure 5. $\mathcal{R}_0$ vs the parameter θ_0.

As a result of Figures 4 and 5, R_0 decreasing when θ increases, and increases whenever θ_0 increase respectively. This finding suggested that effective stay at home intervention have been mitigates the COVID-19 spread, conversely the ineffectiveness of this intervention measure can rising its spread.

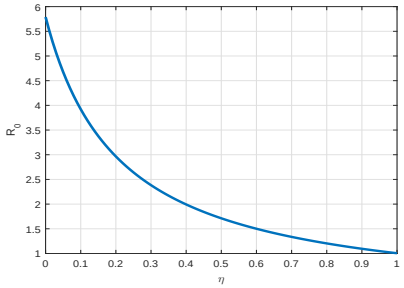

Figure 6. $\mathcal{R}_0$ vs the parameter η.

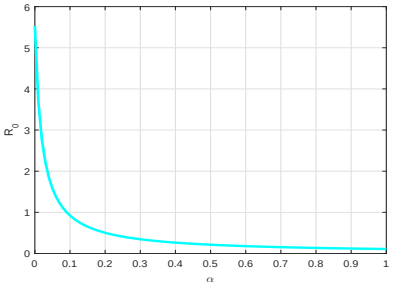

Figure 7. $\mathcal{R}_0$ vs the parameter α.

Figures 6 and 7, show that the increment of η or α can reduce $\mathcal{R}_0$. That is to say, effective quarantine of incubated and infectious individuals can reduce the opportunity of disease spreading.

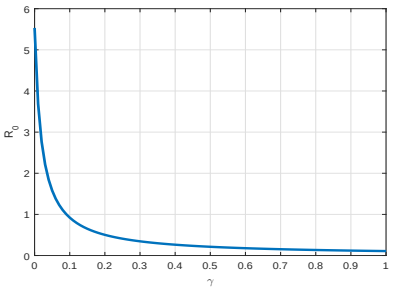

Figure 8. $\mathcal{R}_0$ vs the parameter γ.

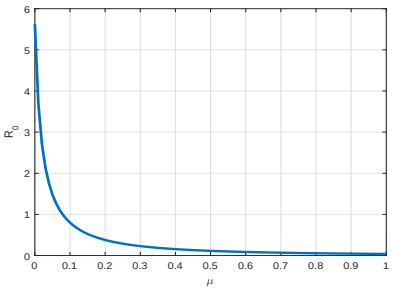

Figure 9. $\mathcal{R}_0$ vs the parameter μ.

From Figures 8 and 9, we find that, short average time from the symptom onset to recovery or death γ and large value of μ can reduce the COVID-19 spread.

4. Numerical results and analysis

In this section, numerical simulation of the model (1) demonstrated. Numerical solutions obtained by using *ode45* package which used to solves systems of ODEs.

The simulation study explores the impact of prevention and control against the spread of the COVID-19 outbreak. The general dynamics, dynamical solution of equilibria, and impacts of prevention and control strategies are under consideration in this section discussion.

4.1 *General dynamics*

We numerically illustrate the asymptotic behavior of the model (1). We take the the initial conditions $S(0) = 0.9,\ Q(0) = 0,\ E(0) = 0.06,\ A(0),\ I(0) = 0.04,\ L(0) = 0,\ R(0) = 0$, and $D(0) = 0$.

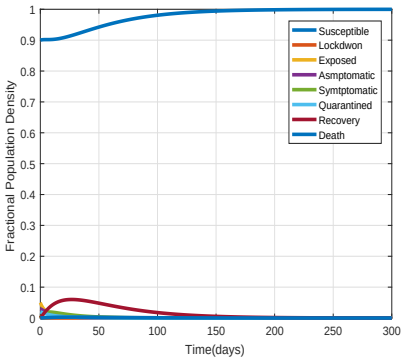

Figure 10. Evaluation of general dynamic for $\mathcal{R}_0 = 0.6355$.

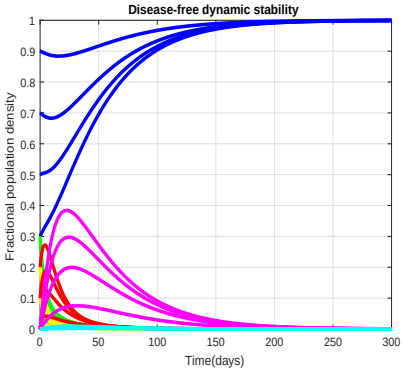

Figure 11. Evaluation of general dynamic for $\mathcal{R}_0 = 0.6355$ and varying initial values.

Consider system (1) with parameters $\beta = 0.05,\ \theta = 0,\ \sigma = 0.1923,\ \alpha = 0,\ \gamma = 0.0714,\ \mu = 0.01,\ \theta_0 = 0.0$. Then, it follows by certain calculations that the threshold $\mathcal{R}_0 = 0.5842$, which is below unity, thus Theorem 3.1 ensures that the disease-free equilibrium E_0 is globally asymptotically stable. For numerical simulation we set initial values as $S(0) = 0.9, E(0) = 0.05, A(0) = 0.02, I(0) = 0.03, Q(0) = L(0) = R(0) = D(0) = 0$. Figure 10 shows the evolutions of state variables, from which it can be observed that the percentages of non-susceptible stat variables population density finally converge to the constant zero, when susceptible population density converge to unity. This means that COVID-19 pandemic would finally tend to extinction and is in agreement with Theorem 3.1. Figure 11 shows the plot of several solutions of system (1) with different randomly-given initial values. It can be seen in Figure 11, that all of these solutions eventually converge to the disease-free equilibrium E_0, which is also consistent with Theorem 3.1.

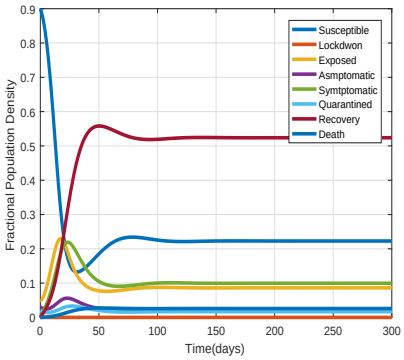

Figure 12. Evaluation of general dynamic for $\mathcal{R}_0 = 3.813$.

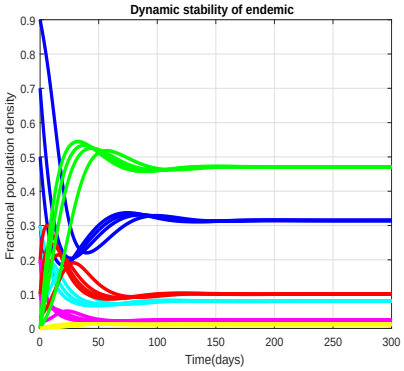

Figure 13. Evaluation of general dynamic for $\mathcal{R}_0 = 3.813$ and varying initial value.

Consider system (1) with parameters $\beta = 0.8$, $\theta = 0$, $\sigma = 0.1923$, $\alpha = 0$, $\gamma = 0.0714$, $\mu = 0.01$, $\theta_0 = 0.0$. Figure 12 shows the time evolutions of state variables which approach to the constants $0.223, 0.0, 0.0862, 0.01626, 0.0259, 0.0996, 0.524$ and 0.0259, respectively. The simulation illustrates the disease spread to peak and keep propagating through the community at a steady level. Figure 13 shows the plot of its four solutions with varying initial values. It can be seen that all of these solutions finally tend to the endemic equilibrium E^*. This result confirms that the endemic equilibrium is asymptotically stable whenever $\mathcal{R}_0 > 1$.

4.2 *Impact of the transmission rate*

The parameter β describes the probability that a susceptible individual converts to be an exposed class by a single infected individual per unit time. The impacts of β on the susceptible, contagious, and deceased population will illustrate.

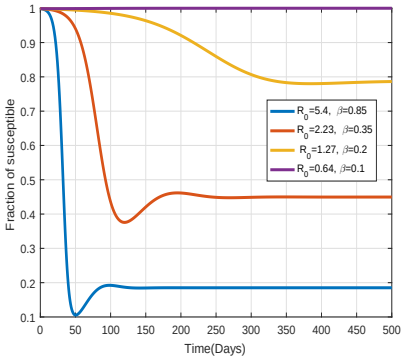

Figure 14. Evaluation of susceptible population.

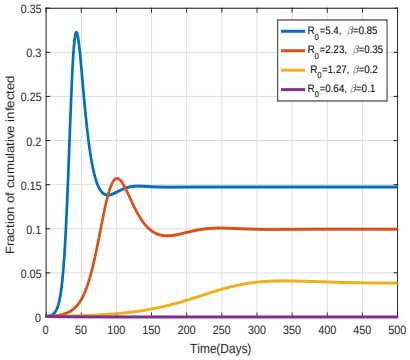

Figure 15. Evaluation of contagious population.

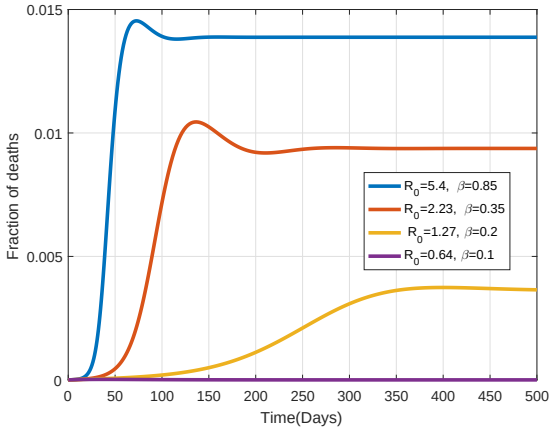

Figure 16. Evaluation of deceased population.

Consider system (1) and set the value of $\beta = 0.85, 0.35, 0.2, 0.1$. From Figure 14 to Figure 16, illustrates that the change of β leads to the uncertainty behavior of the system. It can be seen in Figures 14, 15 and 16 that all these curves ultimately converge to corresponding equilibria, respectively. The final percentage of susceptible will remain stable at a higher level when the value of the parameter β is lower. While the evolutions of the contagious, and deceased population will steady at a higher value when β value high. The simulation designates that

reducing contact transmission (β) treats to control COVID-19 propagation.

In the absence of intervention measures with $\mathcal{R}_0 = 5.4$, near to 90%, susceptible population are being exposed to COVID-19 outbreak and 1.4% of deaths globally this year. The 59% and 76.5% reduction of effective contact transmission provided that, 25% and 60% reduction of the susceptible population exposedness respectively. Also, 35.7% and 71.43% of death reduction obtained by 59% and 76.5% discount of the transmission rate of β. Extensive countermeasures are required to reduce person-to-person transmission of COVID-19. Appropriate care and endeavors to protect or reduce transmission should be involved in the susceptible population.

4.3 *Impact of lockdown*

The impact of a lockdown on the contagious and deceased population will be simulated.

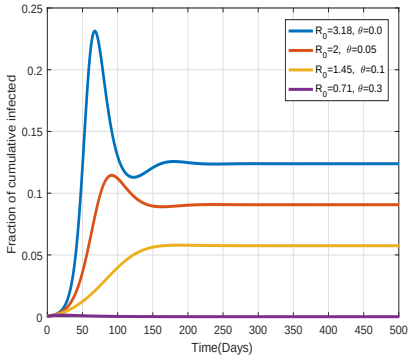

Figure 17. Evaluation of contagious population by varying θ .

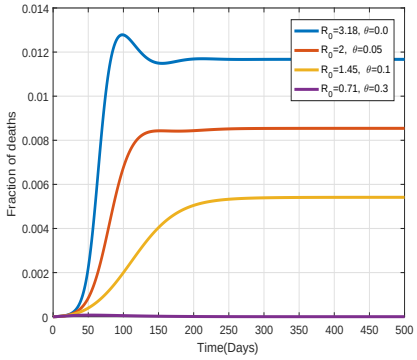

Figure 18. Evaluation of deceased population by varying θ .

Considering system (1) and the transmission rate $\beta = 0.5$. We observe the impact of lockdown by setting the value of $\theta = 0.0, 0.05, 0.1, 0.3$. Figures 17 and 18 show that the impact of θ on infection and deceased case densities of the model. The lockdown coverage rises from 5% to 10%, new infectiousness also reduced from 26.82% to 53.62% after 7 months respectively. Similarly, deceased density also reduce by 26.86%, 53.65% and finally it tends to zero (see Figures 17 and 18). The simulation provides, more than 30% of lockdown coverage with a minimum of 30% efficiency could control the COVID-19 outbreak. Strict social distancing measures were effective in reducing incidence and mortality rates.

4.4 *Lockdown lifting impact*

Restricting mass gathering or lockdown has an impact on the daily life activities of every individual. The impact of lockdown relaxes, or intervention lifting on the spread of COVID-19 will be represented.

Considering system (1)and the transmission rate $\beta = 0.5$ and $\theta = 0.4$. We observe the impact of lockdown return by setting the value of $\theta_0 = 0.0, 0.05, 0.1, 0.7$. Figures 19 and 20 illustrate that the impact of θ_0 on contagious and deceased case densities of the model. In the absence of lockdown lifting, the contagious curve persists at disease-free equilibrium when $\mathcal{R}_0 = 0.56$. The lockdown lifting rises from 5% to 70% new infectiousness also increases from 3.412% to 11.42% after a year respectively.

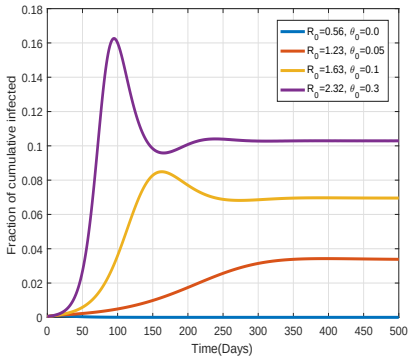

Figure 19. Evaluation of contagious population by varying θ_0.

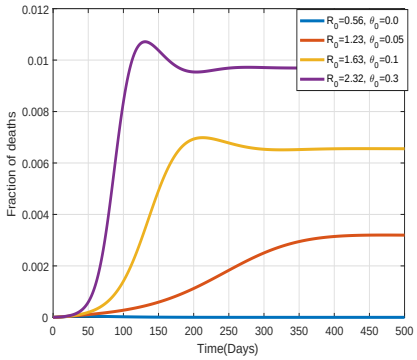

Figure 20. Evaluation of deceased population by varying θ_0.

Similarly, death percentage increase from 0.396% to 1.078% (see Figures 19 and 20. In the absence of other interventions, the result provides more than 5% lifting of lockdown leads the second COVID-19 outbreak prevalence.

4.5 *Impacts of quarantine*

Study the recommended containment strategies of the pandemic, we conduct some numerical simulations to show the contribution of quarantine. Here, we observe the isolation of exposed and infected individuals within different rate:

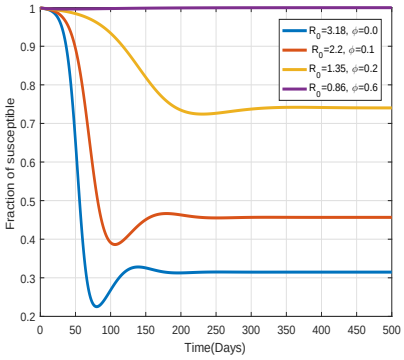

Figure 21. Evaluation of susceptible population.

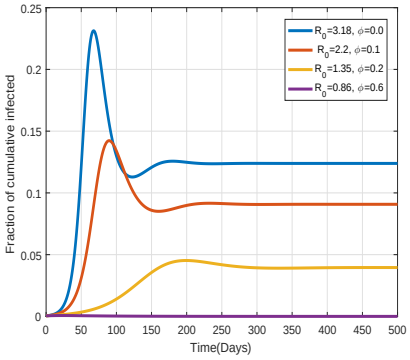

Figure 22. Evaluation of contagious population.

Considering system (1) and the rate $\beta = 0.5$ and $\theta = 0.4$. We observe the impact of exposed quarantine by setting the value of $\phi = 0.0, 0.1, 0.2, 0.6$. It can be observed in Figures 21, 22, and 23 that the impact of ϕ on the susceptible, contagious, and decease population. In the absence of exposed quarantine, 70% of the susceptible population will be exposed to COVID-19. And also, near to 1.2%, will die, when $\mathcal{R}_0 = 3.18$ in this year. Figure 22 displays the new infection population density decreases when the diagnosis and tracing process rises. Similarly, the deceased number decrease when the quarantine coverage of exposed increases (see Figure 23). The result suggests that more than 60% of quarantine of exposed individuals reclines $\mathcal{R}_0$ below one, this implies that COVID-19 spread will be under control.

Now, the impacts of symptomatic infected isolation will be evaluated.

Considering system (1) with the transmission rate $\beta = 0.5$, and by setting the value of $\alpha = 0.0, 0.1, 0.3, 0.5$. It can be observed in Figures 24, 25, and 26 that

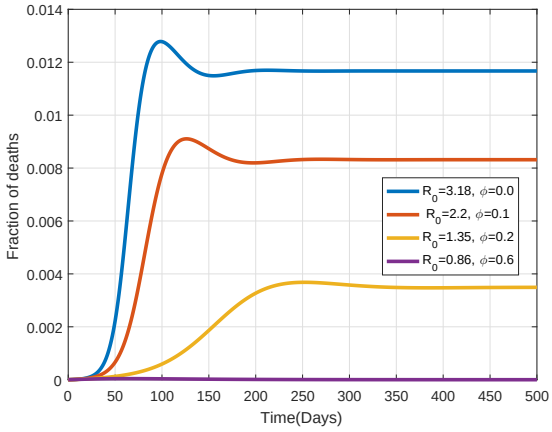

Figure 23. Evaluation of deceased population.

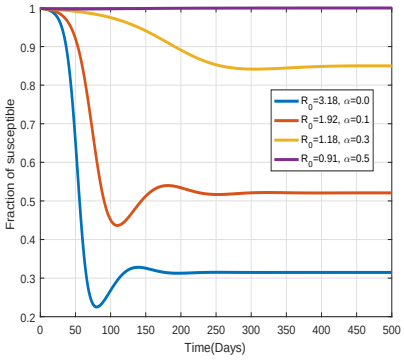

Figure 24. Evaluation of susceptible population.

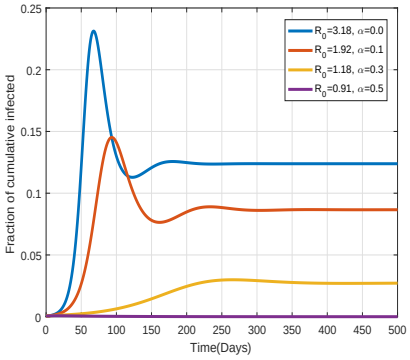

Figure 25. Evaluation of symptomatic infected population.

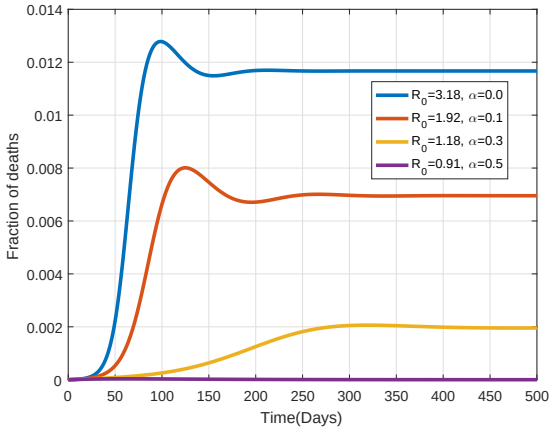

Figure 26. Evaluation of deceased population.

the impact of α on susceptible, infected, and deceased population density. In the absence of isolation of symptomatic infected, 70% of the susceptible population being exposed to COVID-19, and near to 1.2% will die, when $\mathcal{R}_0 = 3.18$ in this year. Figure 25 displays high coverage of isolation monitoring conquers the growth of new symptomatic infected populations. Similarly, the deceased number decrease when isolation rate increases(see Figure 26). The simulation indicates that more than 50% isolation of symptomatic infected individuals defeat $\mathcal{R}_0$ below one, this implies that COVID-19 spread will be under control.

5. Conclusions

The control, containment, mitigation, and pleasant elimination of the coronavirus pandemic requires the rapid and compatible implementation of control and mitigation strategies. Mathematical models are central to this effort but certain issues have to be considered and measured for increased efficacy in their application. The researcher develops a new $SEIR$ type compartmental model it provides insight into the transmission dynamics of COVID-19 with control measures. The model incorporates asymptomatic and symptomatic infected with the modification parameter. The sensitivity analysis gives insight that high contact transmission has a positive impact on secondary infection reproduction of COVID-19. Furthermore, lifting of intervention also accelerates the new infectiousness rate. For suspension and mitigation of COVID-19 spread, appropriate implementation of lockdown and quarantine incredibly valuable.

Numerical simulations are conducted aim to support theoretical analysis and shows the significance of public health intervention to containment these pandemics. The general dynamics of the model with time is illustrated that the disease is die out when $\mathcal{R}_0 \leqslant 1$ (see Figure 10), but its persists in the community whenever $\mathcal{R}_0 > 1$ (see Figure 12). Moreover, socioeconomically crisis caused by these pandemic can be minimized and eliminated when we implemented appropriate control measure.

References

[1] R. M. Anderson and R. M. May, Population biology of infectious diseases, Part I. Nature, **280** (1979) 361-367.
[2] L. Bertolaccini and L. Spaggiari, The hearth of mathematical and statistical modelling during the Coronavirus pandemic, Interactive CardioVascular and Thoracic Surgery, **30** (2020) 801-802.
[3] F. Brauer and C. Castillo-Chavez, Mathematical Models in Population Biology and Epidemiology, Springer, New York, (2012).
[4] T. M. Chen, J. Rui, Q. P. Wang, Z. Y. Zhao, J. A. Cui and L. Yin, A mathematical model for simulating the phase-based transmissibility of a novel coronavirus, Infectious Diseases of Poverty, **9** (2020) 1-8.
[5] Coronavirus disease (COVID-2019) situation reports 85 Available at: `https://www.who.int/emergencies/diseases/novel-coronavirus-2019/situation-reports`.
[6] E. X. DeJesus and C. Kaufman, Routh-Hurwitz criterion in the examination of eigenvalues of a system of nonlinear ordinary differential equations, Physical Review A, **35 (12)** (1987) 5288-5290.
[7] O. Diekmann and J. A. P. Heesterbeek, Mathematical Epidemiology of Infectious Diseases: Model Building, Analysis and Interpretation, John Wiley & Sons, (2000).
[8] H. W. Hethcote, The mathematics of infectious diseases, SIAM Review, **42 (4)** (2000) 599-653.
[9] D. S. Hui et al.,The continuing 2019-nCoV epidemic threat of novel coronaviruses to global health – The latest 2019 novel coronavirus outbreak in Wuhan, China, International Journal of Infectious Diseases, **91** (2020) 264-266.
[10] W. O. Kermack and A. G. McKendrick, A contribution to the mathematical theory of epidemics, Proceedings of the Royal Society of London. Series A, **115** (1927) 700-721.
[11] A. J. Kucharski et al., Early dynamics of transmission and control of COVID-19: a mathematical modelling study, The Lancet Infectious Diseases, **20 (5)** 2020 553-558.
[12] D. K. Mamo and P. R. Koya, Mathematical modeling and simulation study of $SEIR$ disease and data fitting of Ebola epidemic spreading in west Africa, Journal of Multidisciplinary Engineering Science and Technology, **2 (1)** (2015) 106-114.
[13] K. Prem et al., The effect of control strategies to reduce social mixing on outcomes of the COVID-19 epidemic in Wuhan, China: a modelling study, The Lancet Public Health, **5 (5)** (2020) e261-e270.
[14] P. Van den Driessche and J. Watmough, Reproduction numbers and sub-threshold endemic equilibria for compartmental models of disease transmission, Mathematical Biosciences, **180 (1-2)** (2002) 29-48.
[15] WHO. How does COVID-19 Spread? Available at: `https://www.who.int/news-room/q-a-detail/q-a-coronaviruses`.

[16] WHO. What are the symptoms of COVID-19? Available at: https://www.who.int/news-room/q-a-detail/q-a-coronaviruses.
[17] WHO. What is Cornovirus? Available at: https://www.who.int/news-room/q-a-detail/q-a-coronaviruses.
[18] WHO. What is COVID-19? Available at: https://www.who.int/news-room/q-a-detail/q-a-coronaviruses.
[19] D. Wu, T. Wu, Q. Liu and Z. Yang, The SARS-CoV-2 outbreak: what we know, International Journal of Infectious Diseases, **94** (2020) 44-48.
[20] C. Yang and J. Wang, A mathematical model for the novel coronavirus epidemic in Wuhan, China, Mathematical Biosciences and Engineering, **17** (2020) 2708-2724.
[21] J. A. Yorke, Invariance for ordinary differential equations, Mathematical Systems Theory, **1** (1967) 353-372.